https://doi.org/10.2352/ISSN.2470-1173.2019.9.IMSE-371

METHOD FOR THE OPTIMAL APPROXIMATION OF THE SPECTRAL RESPONSE OF MULTICOMPONENT IMAGE

J. Matanga. P. Gouton, E. Bourillot, S. Journaux, P. Ele **,** ***Laboratoire Electronique Informatique et Image (Le2i)(CNRS FRE-2306, Université de Bourgogne***

Abstract

A color image is the result of a very complex physical process. This process involves both light reflectance due to the surface of the object and the sensor. The sensor is the human eye or the image acquisition system. To avoid metamerism phenomena and to give better rendering to the color images resulting from the synthesis, it is sometimes necessary to work in the spectral field. Now, we meet two classes of methods that enable the closest spectral image to be produced from color images. The first method uses circular and exponential functions. The second method uses the Penrose inverse or the Wiener inverse. In this article, we first of all describe the two methods used in a variety of fields from image synthesis to colorimetry not to forget satellite imagery. We then propose a new method linked with the neural network so as to improve the first two approximation methods. This new method can also be used for calibrating most of color digitization systems and sub wavelengths color array filters.

INTRODUCTION

The images used have three components, which cover generally the visible spectrum of the visible light. In most cases, this type of image is sufficient to resolve the problems met. But there are specific cases in which more than three components are required.

It is necessary to have a good command of the acquisition system in the following cases:
-When images are acquired outdoors. Thus aerial images under a clear sky are different from those taken under a cloudy sky. -When the object of study presents spectral information beyond the visible (example of certain plants that emit in infrared). -When it is necessary to acquire an image with greater precision so as to avoid any confusion between the different color hues. -When the Lab or Luv space is to be used, it is essential to know the composition of the reference white. -Finally, when it is necessary to calibrate the acquisition system.

To bring some solutions of the above-mentioned problems, we propose to tackle in this article the complex question linked with the color image acquisition system. We propose a comparative study of spectral reflectance retrieval by different methods and we then propose a new method linked with the neural network.

In this paper, we will describe the method that is now used for the reconstruction of the spectral response of a multi-component image. This technique can be extended to the calibration of any other digitization system.

Finally, the last part will be dedicated to our spectral response reconstruction method based on neural networks. A comparative and objective analysis will lead us towards the best method depending on the color problem to be solved.

Reconstruction of the spectral response of an image using exponential functions

Overview of this method

The integral relation described in equation (1) is a simplification of the physical phenomena involved in the lighting of an object. This observation is an established fact since the light interference phenomena have been discovered but often neglected. The work carried out by Smits and Meyer [23] was a precursor in the field. They tried to simulate the interference phenomena so as to take them into account the color rendering. This block diagram is composed of the object we wish to see. This object is characterized by its spectral reflectance s_λ It is illuminated by a light L_λ coming from a point source. Consider any observer; if a monochromatic light produces the illumination, all these parameters are constant. On the other hand, for a polychromatic light, these parameters will depend on the wavelength λ. This phenomenon has been formed in equation as:

$$v_i = k \int_{\lambda_{min}}^{\lambda_{max}} L(\lambda)s(\lambda)f_i(\lambda)d\lambda \quad (1)$$

s is the spectral reflectance of the object observed and f_i represents one of the basic functions of the CIE. If $\bar{x}$, $\bar{y}$, $\bar{z}$ are the basic functions, the CIE proposes an XYZ colorimetric base that connects the spectral response of the object with the observer response according to equations (2), (3), (4):

$$X = k \int_{\lambda_{min}}^{\lambda_{max}} L(\lambda)s(\lambda)\bar{x}(\lambda)d\lambda \quad (2)$$

$$Y = k \int_{\lambda_{min}}^{\lambda_{max}} L(\lambda)s(\lambda)\bar{y}(\lambda)d\lambda \quad (3)$$

$$Z = k \int_{\lambda_{min}}^{\lambda_{max}} L(\lambda)s(\lambda)\bar{z}(\lambda)d\lambda \quad (4)$$

k is a constant, which is obtained by using a white reference.
In 1989, A.S. Glassner [7] proposed a solution that allows the transformation of a color image into a spectral image. The aim of this work was to have a tool capable of generating a spectral correspondence from drawings. It forms the foundation of the spectral reconstruction of color images.

We were trying to match a triad (R, G, B) with its spectral distribution. In order to succeed, we started with a transformation that allows the passage from the RGB space to the XYZ space of the CIE.

Given Lλ and sλ which respectively symbolize the illumination and the reflectance of the object to be visualized and depend on the wavelength. If we are only interested in the visible range, the color v is defined by the fundamental relation (see equation 1).

The color is defined in a three-dimensional space (3D). To obtain a bijective relation between the color and its spectrum, three basic functions g_j are determined that could fully describe this spectrum. Consequently, any spectral density can then be described through the knowledge of these basic functions g_j and coordinates a_j so that (5):

$$\phi_\lambda^* = \sum_{j=1}^{3} a_j g_j \quad (5)$$

with: $\phi_\lambda^* = s_\lambda L_\lambda$
By replacing ϕ_λ^* with its value in the equation (1), we achieve the relation (6):

$$v_i = k \int_{\lambda min}^{\lambda max} \sum_{j=1}^{3} a_j g_j(\lambda) f_i(\lambda) d\lambda \quad (6)$$

If we render k discrete, we arrive at relation (7):

$$v_i^* = k \sum_{\lambda min}^{\lambda max} \sum_{j=1}^{3} a_j g_j(\lambda) f_i(\lambda) \Delta\lambda \quad (7)$$

A matrix version is given below (8)

$$\begin{pmatrix} v_1 \\ v_2 \\ v_3 \end{pmatrix} = \begin{bmatrix} h_{11} & h_{12} & h_{13} \\ h_{21} & h_{22} & h_{23} \\ h_{31} & h_{32} & h_{33} \end{bmatrix} \begin{pmatrix} a_1 \\ a_2 \\ a_3 \end{pmatrix} \quad (8)$$

v = H.a
with:

$$h_{ij} = k \sum_{\lambda min}^{\lambda max} g_j(\lambda) f_i(\lambda) \Delta\lambda \quad (9)$$

where $\Delta\lambda$ represents the spectral resolution. It can be admitted that these basic functions meet some constraints according to the CIE recommendation, and Morovic and Finlayson works:
-They should be linearly independent. –They should be maximum for the red, the green and the blue wavelengths, which are defined be: λ_r, λ_g, λ_b.

We calculate the error committed in rebuilding the reference color coming from Macbeth color chart (called also "Macbeth Color Checker") as well as the spectral relation by the relation (10, 11) below:

$$\Delta v = \frac{1}{3} \sum_i \sqrt{\frac{(v_i - v_i^*)^2}{v_i^2}} \quad (10)$$

with i=1, 2, 3.

$$\Delta\phi = \frac{1}{J} \sum_{i=1}^{J} |\phi_i - \phi_i^*| \quad (11)$$

J represents the total number of spectral data given by equation (12) (the approached integer value):

$$J \approx \frac{\lambda_{max} - \lambda_{min}}{\Delta\lambda} \quad (12)$$

v_i is the initial color and ϕ its spectral stimulus function related with reflectance light. ϕ^* is the color stimulus function calculated with the relation (5) and v_i^* is obtained by using the relation (7).

To have a basis for comparison, we used the Macbeth color chart. The Macbeth color chart is less rich than that of Munsell. It is composed of 24 colors numbered from 1 to 24. Each color is characterized by its three components RGB and its spectral response. The spectral response of each color was carried out by a spectroradiometer. These data are standard and more especially used for calibration.

Figure (1) shows the different colors of the Macbeth color chart.

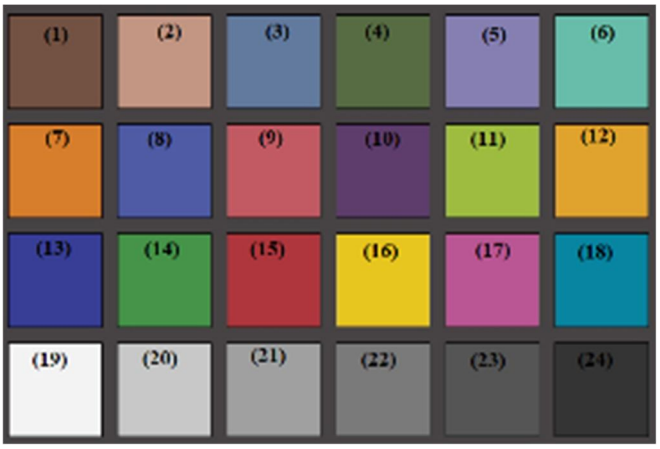

Figure 1. Colors of the Macbeth color chart

Gaussian function

Although the introduction of circular functions has brought in certain richness at spectral resolution level, this representation is still far from the real color spectrum. The faithful reproduction of the color is difficult to reach. Maloney and al [14], Peercy [19], propose a solution using Gaussian functions. A comparison between circular and Gaussian function has done by Peercy and a deep analysis shows that these methods seem to be similar. Here, we prose to summarize the Gaussian method.

The main reason was to approximate the spectral reflectance by simulating the spectral response of the photosensitive sensors so as to make their model adhere to physical reality. Peercy proposes to use Gaussian functions as basic functions focused on the primary colors RGB. This choice is not unimportant because the spectral responses of the red, green and blue filters used in cameras have allure close to the Gaussian and are focused. The equations (13) characterize these basic functions.

$$\left.\begin{aligned} g_1 &= e^{-ln2\left(2\frac{\lambda-\lambda_r}{\sigma_1}\right)^2} \\ g_2 &= e^{-ln2\left(2\frac{\lambda-\lambda_g}{\sigma_2}\right)^2} \\ g_3 &= e^{-ln2\left(2\frac{\lambda-\lambda_b}{\sigma_3}\right)^2} \end{aligned}\right\} \quad (13)$$

The parameters σ_i allow the color effect to be taken into account, whether or not it is saturated. They are calculated by the relation (14):

$$\left.\begin{aligned} \sigma_1 &= \xi_{12}\omega_{min} + (1-\xi_{12})\omega_{max} \\ \sigma_2 &= \xi_{23}\omega_{min} + (1-\xi_{23})\omega_{max} \\ \sigma_3 &= min(\sigma_1, \sigma_2) \end{aligned}\right\} \quad (14)$$

with: $\xi_{12} = \frac{|v_r - v_g|}{v_r + v_g}$ and $\xi_{23} = \frac{|v_g - v_b|}{v_g + v_b}$.
The constants ω_{min} and ω_{max} (respectively 10 nm and 150 nm) are obtained empirically. v_r, v_g, v_b are red, green and blue primary colors. The figure (2) shows an example of spectral reconstruction starting from basic Gaussian functions. We used the color number 11 in the Macbeth color chart base defined in figure (1).

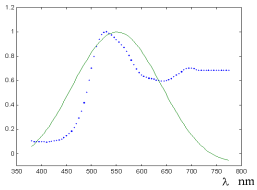

Figure 2. Spectral reconstruction using Gaussian functions. A dotted line shows the initial spectrum; a solid line shows the rebuilt spectrum (R=173, G=187, B=78; N°11;$\Delta\phi$ = 27.06%)

Results are better for the wave lengths near the blue and diverge toward the red. Although the global result is satisfactory, it can be seen that the error on the rebuilt spectrum remains high. These errors can be the cause of the metamerism phenomena met in colorimetry. That is why, in the rest of this paper, we shall propose works based on physical reality.

Setting up of an equation of the multi-component image acquisition system

Proposal

Compared to the previous method, the image is obtained by an electronic acquisition system. The acquisition system is composed of: the object to be observed, an illumination, a set of filters, the optics, the camera and finally a PC equipped with an acquisition card.

We consider that the acquisition system is characterized by optical properties Γ_λ,$\Phi_{i\lambda}$ the spectral filter blocked on the wavelength of the primary λ_i (or any other frequency of the studied spectrum) and photosensitive properties W(λ). The object is illuminated by a polychromatic light [8], [20], [24]. By generalizing the relation defined by the equation (1), we obtain the discrete relation (15):

$$v_i = k\sum_{\lambda min}^{\lambda max} L(\lambda)s(\lambda)\Gamma(\lambda)W(\lambda)\Phi_i(\lambda)\Delta\lambda \qquad (15)$$

The number of filters may vary from 1 (monochrome image) to N. The larger N is the better is the spectral or colorimetric resolution. For a standard color image N=3.

If we take H= [L, Γ , W, Φ_i ...] then the relation (15) leads to the matrix equation (16) for one color:

$$v = H.s \qquad (16)$$

H is often unknown, which represents the acquisition system with which the illumination is associated. v= [v1, v2, …vN]^T represents the colour vector for a space with N dimension. s=[s1,s2,..,sJ]^T is the spectral density of the studied object. As the object is composed of just one colour, it is impossible to identify H. We generally use the Munsell color atlas [8] or the Macbeth colour chart. For this work, we arbitrarily use the Macbeth color chart. This chart is composed of 24 colours, we obtain a system of 24 equations with x unknowns (x is equal generally 80 for a best spectral resolution from 400 to 800 nm).

Equation (16), which is true for one object, can be rewrite as equation (17) below for K objects (colors nuances):

$$V = H.S \qquad (17)$$

V is a matrix which has the dimension NxK (K= total number of different colors).

S is a matrix which has the dimension JxK (J defined by the relation 12), represents all the spectral reflectances of the chart.

H has the dimension NxJ.

The advantage of using the Macbeth colour chart is that we know the spectral response s of each colour in the data base; therefore, from the colour vectors v obtained via the acquisition system, we resolve our system to find H. Consequently, we can identify our acquisition system if the light is properly defined. This results in the relation (18):

$$H=V.S^\circ \qquad (18)$$

The matrix S° is the generalized of the matrix S. If S is a square and non singular then:

$S^\circ=S^{-1}$.

To find H in most cases, we shall analyse two types of approach: either through an approached inverse matrix or by a neural approach.

Identification of H via the matrix method

Pseudo-inverse matrix

Matrix S (composed of all the spectral responses of the color contained in the Macbeth color chart) is not simply non-singular. Such as defined, our system does not allow any solution or infinity of solutions. Most of the methods proposed tend towards the optimal solution. Thus, the singular decomposition values are one of them.

We recall here that the notion of inverse applies to square matrices if the columns (rows) of this matrix are linearly independent. When it exists, this inverse is unique for a given matrix. Thus, Moore (1920) proposes to extend this notion of inverse to the matrices not included in the above category [2], [8]. Later, Penrose when resuming Moore's work proposed the generalized inverse matrix called Penrose inverse or pseudo-inverse matrix. The algorithm of generalized inverse matrix is given by relation (19).

$$\Sigma^\circ = \begin{bmatrix} \delta^{\frac{1}{2}} & O_1^T \\ O_2^T & O_3 \end{bmatrix} \qquad (19)$$

The error on the calculation of $\Delta\phi$ is defined in the relation (11). We employed this method to rebuild the whole system used to acquire data from the Macbeth colour chart. Figure (3) shows the appearance of the system represented by H. The three components RGB lead to three functions $H_i(\lambda)$.The curves H show the spectral response of the whole formed by the spectral acquisition system (spectroradiometer) and the illuminating light. Figure (4) gives the standardized spectral density and its approximation for the colour defined in figure (1).

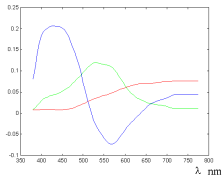

Figure 3. Modelling of the acquisition system And the illumination(R, B, G)

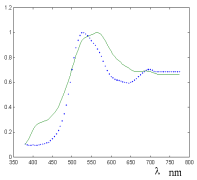

Figure 4. Spectral density rebuilt from the penrose inverse

The initial spectrum is a dotted; the rebuilt is solid line (R=173; G=187; B=78; N°11; $\Delta\phi$=9.65%).

The Penrose inverse introduces noise that increases the difference between the real spectrum and the calculated spectrum. There are solutions to limit the noise. The first one consists in limiting the number of Eigen vectors. This increases the gap between the real spectrum and that sought for. The solution used here is based on the principle of linear hetero-associative memories. The hetero-associative memory is a neural network that uses the Penrose inverse to calculate the real response knowing the theoretical response. This method is very interesting since it allows the gap between the real spectrum and the rebuilt spectrum to be reduced. This method was preferred to the first solution that consists in drastically reducing the number of Eigen values. Nevertheless it does not converge towards a global minimum.

Wiener inverse

The method we have just seen gives some good results, but it is noisy. Other methods are often used to reduce this noise. Research workers such as PG Herzog and his team [9] use the smooth inverse called of the Wiener inverse.

Let us note that S^L, the smooth inverse or the Wiener inverse of matrix S, S^L is calculated by the relation (20):

$$S^L = (M^{W2})^{-1}.S^T.(S.(M^{W2})^{-1}.S^T)^{-1} \quad (20)$$

With: $M^{W2} = M^{W1} + \varepsilon I$.

M^{W1}, a matrix introduced by Mancill [15] is equal to the relation (21) and this matrix is singular. So as to be able to inverse it, it is altered by εI where I is the identity matrix and ε a very small value.

$$M^{w1} = \begin{bmatrix} 1 & -2 & 1 & 0 & \dots & \dots & \dots & \dots & \dots \\ -2 & 5 & -4 & 1 & 0 & \dots & \dots & \dots & \dots \\ 1 & -4 & 6 & -4 & 1 & 0 & \dots & \dots & \dots \\ 0 & 1 & -4 & 6 & -4 & 1 & 0 & \dots & \dots \\ \dots & : & : & : & : & : & : & : & : \\ \dots & \dots & 0 & 1 & -4 & 6 & -4 & 1 & 0 \\ \dots & \dots & \dots & 0 & 1 & -4 & 6 & -4 & 1 \\ \dots & \dots & \dots & \dots & 0 & 1 & -4 & 5 & -2 \\ \dots & \dots & \dots & \dots & \dots & 0 & 1 & -2 & 1 \end{bmatrix} \quad (21)$$

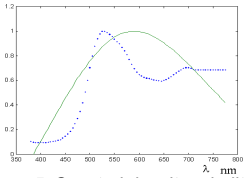

Figure 5. Spectral density rebuilt from the inverse of Wiener

The initial spectrum is a dotted line; the rebuilt spectrum is a solid line

(R=173 G=187 B=78; N° 11; $\Delta\phi$ = 17.93%)

For the chosen color, the reconstruction error is higher (figure 5) than the pseudo-inverse method. But nevertheless, this difference is smaller than the methods using basic Gaussian functions.

It can be noted that the Wiener inverse method is suitable for the reconstruction of very monotonous spectra. Consequently, it is more suitable for colors situated on the achromatic axis.

Approximation of the spectral response by neural learning

All the solutions we have just seen are interesting. But there is still a difference between the initial spectrum and the calculated spectrum. Over recent years, very powerful methods have been developed in the field of pattern recognition. These methods, inspired by neuroscience, are highly efficient mathematical tools. Referring to previous works [10], we propose an extension to the identification of the system represented by matrix H. Indeed, the neural networks are powerful, parsimonious, and universal approximators, for the interpolation of digital data.

Many works exist in the scientific literature which treats the problem of the peripheral calibration (screen, scanner, etc.) [3], [11]. In this part of this article we describe some part of their methods.

Process and method

We use a neural network theory to describe ours process and method. A neural network [1] [4] is composed of elementary integrators or formal neurons (perceptron) and is a succession of two elementary mathematics operators:

-A summation of the input vector xi or stimulus (i=1…I where I is the dimension of the input vector) weighted by coefficients called weights $w_{j,i}$. this sum evaluates the activation potential a_j of the neuron (22):

$$a_j = \sum_{i=1}^{I} w_{j,i} x_i \quad (22)$$

With x_0=1

- A non-linear thresholding operation by activation function F which evaluates the output of the neuron.

This can be schematized by Figure (6) below

$$o_k = F(a_k) \quad (23)$$

The association of several formal neurons will form a layer of neurons (Figure 7). The generalized form of the potential activation vector becomes $A_K = WX_k$ with $w_{j,I}$ the intensity of the connection between the i^{th} input vector and j^{th} neurons. The number of formal neurons varies from 1 to P and

$X_k = [x_0, x_1 \dots x_I]^T$.

$$W = \begin{bmatrix} w_{1,0} & w_{1,1} \cdots & w_{1,I} \\ w_{2,0} & w_{2,1} \cdots & w_{2,I} \\ \vdots & \vdots & \vdots \\ w_{P,0} & w_{P,1} & w_{P,I} \end{bmatrix} \quad (24)$$

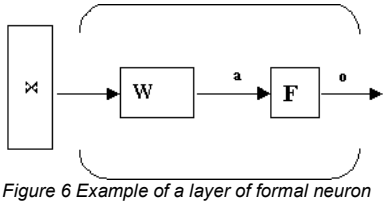

Figure 6 Example of a layer of formal neuron

The vector X of input will be of size I * N where I is the size of the input vector, N is the number of examples or observable.

The most frequently used supervised learning network is the MLP (Multi-Layer Perceptron). It is used in a number of industrial applications [12] for signal and image processing such as form recognition [18]. The architecture of a MLP is composed of the assembly of formal neurons in two or more layers (figure 9).

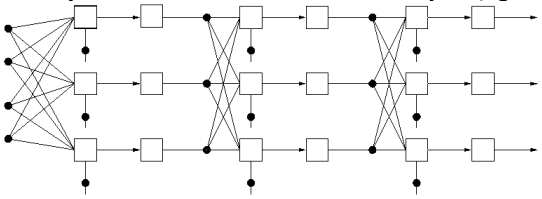

Figure 7. Multi-layer neural network (Multi Layer Perceptron)

The complexity of the network, i.e. the number of layers and the number of neurons per layer, will influence the performance of the interpolation [10].

The network response at output will be evaluated (25) for each example (subscripted k):

$$O_k = F_i\left(W_i \dots F_2\left(W_2\left(F_1(W_1 X_k)\right)\right)\right) \quad (25)$$

with W_i connection matrix of layer i and F_i activation function of layer i, x_k the k^{th} observable.

Supervised learning

The supervised learning procedure will require:

-A learning and test set that will form the data base with dimension N. The network parameters are calculated from the N-N_0 examples formed by the couples {input x_k, theoretical output t_k} of the

learning basis. Many authors have underlined the importance of the learning basis which should be representative of each class and in sufficient number [18] [25].
The performances of the network are established from the N_0 examples of the test basis. The measurement of performance is established by the comparison between the mean square errors of the learning set and the mean square errors of the test set [25]. When the database is very small the validation of the network parameters use the leave-one-out cross validation method [25][26].
- The definition of a cost function that measures the difference between the required theoretical output and the output estimated by the network [5]. The most frequently used cost function is the total cost function (equation 26) of the mean squares or root mean square error, insensitive to its number N of examples [22].

$$J = \frac{1}{2N}\sum_{k=1}^{N} e_k^T e_k$$

equivalent to

$$J = \frac{1}{2N}\sum_{k=1}^{N} (t_k - o_k)^T (t_k - o_k) \quad (26)$$

Where e_k is the instant error vector at network output between the theoretical response vector t_k and the calculated response vector ok of the k^{th} stimulus.
The learning of a network is realised by iteration or epoch. An epoch therefore corresponds with the presentation of all the examples for learning.
- A minimisation algorithm of this cost function in relation to the weight W of the network. The choice of the optimisation method will mainly depend on the complexity of the network, i.e. the size of the connection matrices and input vector [22].

Gradient backpropagation algorithm

We cannot speak of supervised learning multi-layer networks without mentioning the most famous one: the MLP error backpropagation network. This algorithm [13], [21] is a generalisation of the Widrow-Hoff rule (or general delta rule) [4].
The correction of the network weights is defined by the following equation (figure 8, equation 27).

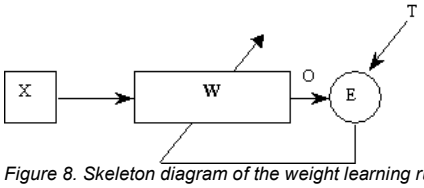

Figure 8. Skeleton diagram of the weight learning rule

$$W_{i+1} = W_i + \Delta W_i \text{ with } \Delta W = \sum_{k=1}^{N} \Delta W_k \text{ and}$$
$$\Delta W_k = -\eta \nabla_w J_k \quad (27)$$

with (η) constant learning rate gradient.

Furthermore, this first order optimisation method does not guarantee the convergence to a minimum of the cost function. The best improvements for minimising the root mean square error for the networks of multi-layer neurones come from the classical optimisation methods for functions with several variables, in particular the digital optimisation methods with no second order constraints such as backpropagation by conjugated gradient, the quasi-Newton algorithm. Using the appropriate optimization method, as the Bayesian Regularization method we defined ours process, and method.

The main reason for choosing the Bayesian Regularization algorithm (BR) is the fact that, it can result in good generalization for difficult, small or noisy datasets. Training stops according to adaptive weight minimization (regularization), the lesser cost of the calculations and the quick guarantee of the convergence to a minimum (28):

$$\Delta W_k = -[G_k]^{-1} \nabla J_k \quad (28)$$

Among the limited neighbourhood methods, the Fletcher method [17] [6] [Dreyfus] was chosen and developed. The Hessian is always positive definite, which ensures the convergence to a minimum of the solution.

Methodology

We used a two-layer network, which is largely sufficient, for the problem considered. The first layer (called hidden layer) is composed of a layer of 15 neurones. The number of points in our spectral response fixes the output layer. With a chosen resolution of $\Delta\lambda$ nm, we actually have 81 points to rebuild. Consequently 81 neurons are necessary on the output layer. This can be schematized by Figure (9) below

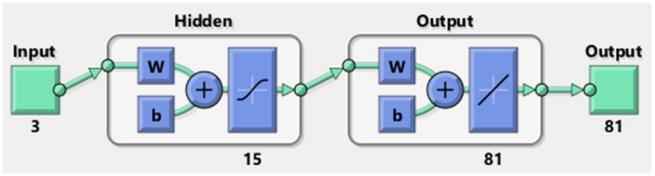

Figure 9. The MLP architecture of the proposed method

Moreover, due to the small database of example, the leave one out cross validation method has been applied [25]. For the learning, we have 18 samples to present to the network and for the testing step, we have 6 samples (Colors 1, 8, 11, 16, 18 and 20) of the Macbeth color chart. Each input datum puts in a vector of 3 components. The activation function of the input layer is a sigmoid function whereas we have a linear activation on the output layer. After the learning stage, we keep the weight matrices W_1, W_2 and the activation thresholds B_1 and B_2. These 2 matrices and the 2 associated vectors represent the system to be identified. Therefore, starting from any triplet, whether or not it is in the Macbeth colour chart, we can deduce its spectral response. Considering the very few filters used, (here red, green and blue) it will always contain approximation errors. The solution we suggest is to increase the number of filters. This solution is conditioned by the place required for storing such an image.

The training set and test set results are shown respectively in the figure (10) and the figure (11)

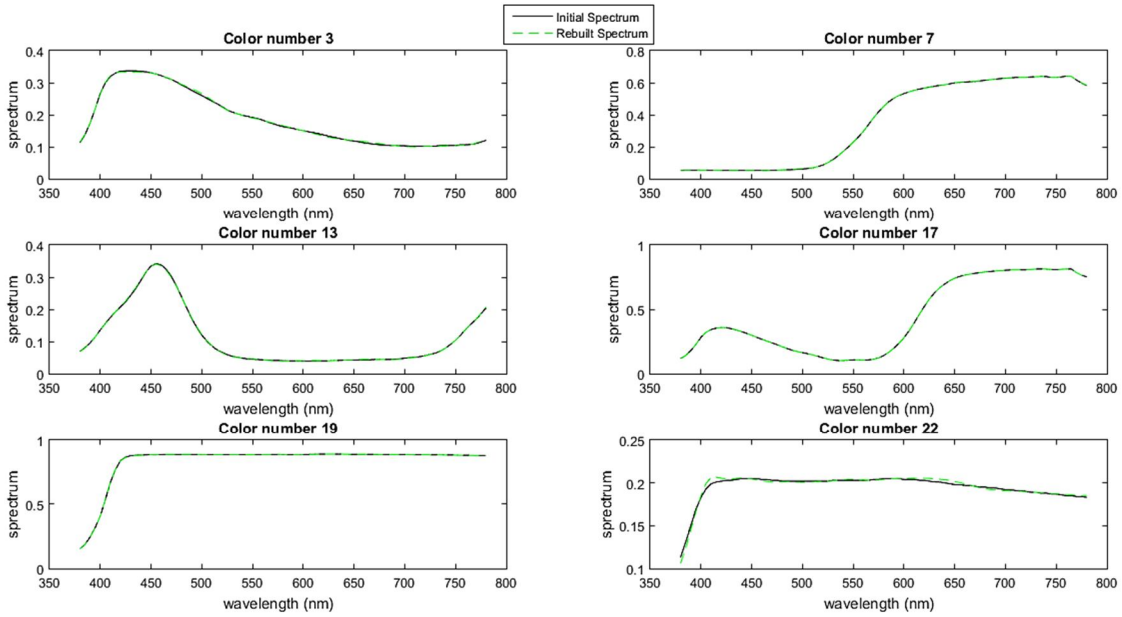

Figure 10. Rebuilt spectral density through learning of a two-layer network for some colors in the Training Set

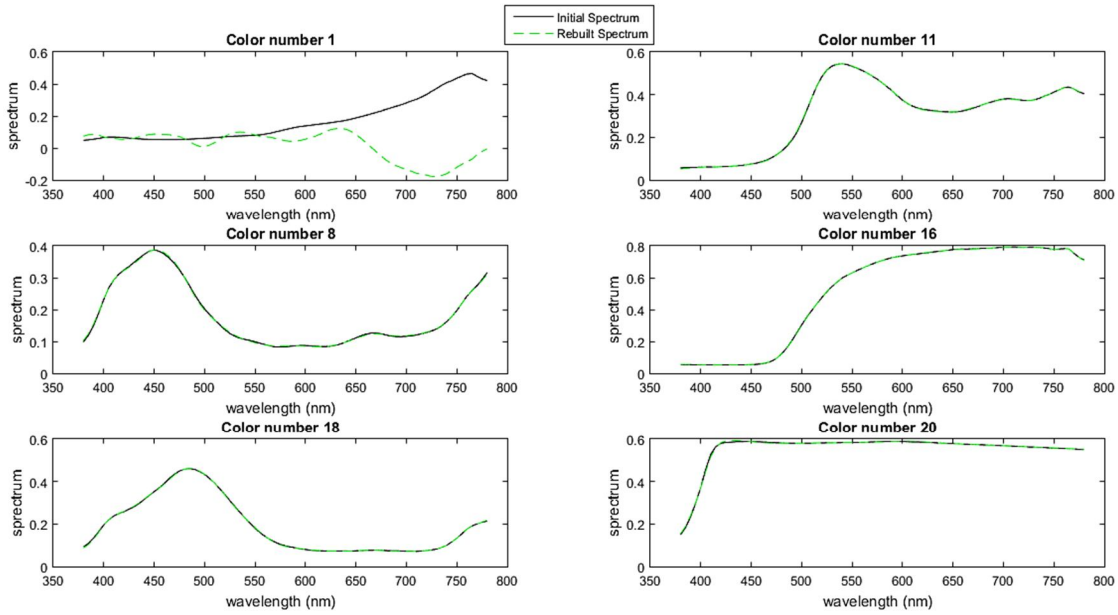

Figure 11. Rebuilt spectral density through learning of a two-layer network for colors in the Test Set

Global results analysis

Overview of this method

For one color, it is difficult to have a proper idea. So as to bring in a deep analysis of the various spectral image reconstruction methods, the comparison is done on the whole color of the Macbeth color chart.

In this analyze, table result show the whole chart color of our database and we can see for each color the RGB components. Table 1-a, table 1-b, give different errors produced by each reconstruction method for each color in the database and table 2 gives the mean error. The another tables which we are not present here gives for each color the initial spectral reflectance in dotted line and the reconstruction spectral using a multi-layer BR (Bayesian Regularization) optimization in solid line. Another table resumes the technical specification used to implement the neuronal learning. The new method we proposed is the best approximation, since it permits to perfectly rebuild the spectral reflectance.

The method uses the Penrose inverse remains acceptable, because it is very fast in time of calculation and permits fast verifications. In our application, to avoid the noise due to this inversion method we preferred a hetero-associative memory with learning rate constant.

For the whole samples which composed the basis for our study, the neural method gives the best results for all samples. This comparative survey spread to the set of the 24 colors gives satisfaction on the proposed scientific approach. Neuronal aspect is not the only element to take in consideration since it has been done by various authors, but here we have brought a deep analyze in the method of optimization and results show that BR approximation is well adapted in this case. Only 24 colors (in our database) is used to rebuild the spectral reflectance, for each color, it produces the best spectral reconstruction with a mean error less than 0.3%. Thanks to the present power computer we can easily implement a 3 layers network neuronal configuration. The learning process takes less than 1 minute CPU times (43 seconds exactly) which seems reasonable. Although in the scientific literature no indication is given on the number of neurons for hidden layers, best results have been obtained with 6 neurons for the layer 1 and 20 neurons for the layer 2. The output layer is constructed with 80 neurons. We observe that the Penrose inverse is second in relation to the other remaining methods. This survey shows that the 3rd position is attributed to the Gaussian basic function approach. Finally the Wiener inverse is worst. This is in contradiction with the author who based their affirmation only on a few chosen colors.

The neuronal network method we proposed requires a long time of learning. In many applications the identification of the system acquisition or visualization is done once. Therefore increase the learning time are necessary for best identification. Otherwise 2 layers can be used in order to reduce the learning time.

Number	1	2	3	4	5	6	7	8	9	10	11	12
ΔS Exponential Function(%)	53.60	41.32	13.18	49.18	30.34	23.30	23.01	18.40	22.62	42.84	27.06	25.37
ΔS Penrose inverse(%)	23.70	9.32	24.05	31.83	13.79	9.70	4.28	18.27	6.03	27.65	11.55	3.61
ΔS Wiener inverse(%)	56.99	48.24	10.57	55.54	31.61	20.83	49.80	13.34	53.93	43.88	36.03	46.68
ΔS BR Neural Network(%)	**2.300**	**0.007**	**0.021**	**1.979**	**0.002**	**0.012**	**0.007**	**0.021**	**0.002**	**0.005**	**0.013**	**0.660**

Table 1-a. Comparison between 4 spectral reconstruction methods applied to color database

Number	13	14	15	16	17	18	19	20	21	22	23	24
ΔS Exponential Function(%)	23.61	31.09	20.75	26.08	22.32	32.57	19.80	19.91	18.89	18.82	20.00	19.34
ΔS Penrose inverse(%)	18.77	15.01	6.87	1.89	4.02	27.24	15.26	17.02	17.90	17.92	17.28	14.18
ΔS Wiener inverse(%)	12.77	39.42	58.42	41.99	47.18	17.47	45.79	44.11	42.82	42.03	42.54	40.47
ΔS BR Neural Network(%)	**0.010**	**0.651**	**0.003**	**0.009**	**0.003**	**0.015**	**0.009**	**0.024**	**0.016**	**0.021**	**0.014**	**0.024**

Table 1-b. Comparison between 4 spectral reconstruction methods applied to color database

Reconstruction Method	Mean spectral estimation error
ΔS Exponential Function(%)	26.81
ΔS Penrose inverse(%)	14.88
ΔS Wiener inverse(%)	39.26
ΔS BR Neural Network(%)	**0.24**

Table 2. Comparison between Mean spectral reconstruction errors for 4 methods

Conclusion

In the image processing chain, the acquisition of these images is a key element of the process. In this paper we have proposed a method based on the neural network so as to improve the spectral response estimation starting from a color triad (or set of filters). This tool is precursor of experimental work allowing improving the quality of multi-component images and acquisition systems.

To the two existing models, we have added a third one:

The first model is used in the field of image synthesis. The image reconstruction method lies on a decomposition of the spectral reflectance in a space of circular functions or exponential functions. The aim of the work is to give the color image a rendering that has no connection with the physical reality of the colors. The reconstruction errors calculated from a choice of color ranges drawn from the Macbeth color chart show that the method using the circular functions is closer to reality. The approach used here is not different from the models below. Consequently, from the real spectral response of the object, we can make it undergo the required transformations.

The second model is used in the field of acquisition of multi-component images called multi-spectral image. The main concern in this field focuses on the colorimetric quality of the objects and on the reproducibility so as to avoid the effects of light and metamerism. This requires the power to model the acquisition system. Two methods were used in this field. One consisted in using the Penrose inverse (singular value method) and the other approach uses the Wiener inverse (or smooth inverse). Out of these two methods, the first one gives the best results on the rebuilt spectrum.

The third model we propose is to exploit the neural approaches that are subjacent in the second model. It is not the first time that the neural networks are used in the identification of systems. We can mention the frequent case in automatism. Considering the complexity of the system to be identified, we have opted for a multi-layer network with backpropagation error. To avoid getting trapped in local minima for the quadratic error, we use second order optimization methods. The Bayesian Regularization method was preferred since our data allowed it and furthermore it converges very quickly (43 seconds), after 243 iterations with 2 layers. The best result is obtained when we increase the learning time and it gives the lowest reconstruction error which is less than 0.09%.

References

[1] Abdi H, "A neural network primer. Journal of Biological Systems", Vol.2(3), p 247-283, 1994.

[2] Abdi H, "Les réseaux de neurones", Presses Universitaires de Grenoble, 1994.

[3] Arai Y., Nakauchi S., Usui S., "Color Correction Method Based on the Spectral Reflectance Estimation using a Neural Network", Color Imaging Conference, pp 5-9, 1996

[4] Bishop C "Neural network for pattern recognition", Oxford University Press, 1995.

[5] Daoudi M, "Classification interactive multidimensionnelle par les réseaux neuronaux et la Morphologie Mathématique", Thèse de Docteur en Productique, Université des Sciences et Technologies de Lille, 1993.

[6] Fletcher R, "Practical Methods of optimisation", John Wiley & Sons, 2nd edition, 1987.

[7] Glassner A.S., "How to derive a spectrum from an RGB Triplet", IEEE Computer Graphics & Applications, vol 9,n°4, pp 95-99.

[8] Hardeberg Y.J, "Acquisition et reproduction d'images couleur: approches colorimétrique et multispectrale", Thèse de Doctorat, ENST, Paris, Janvier 1999.

[9] Herzog P.G., Knipp D, Stiebig H, König F, "Colorimetric characterisation of novel multiple-chnannel sensors for imaging and metrology", Journal of Electronic Imaging vol 8, n°4, pp 332-341, October 1999.

[10] Journaux S, "Evaluation de l'endommagement de pièces métalliques par analyse d'images : endommagement piqûre de corrosion et endommagement par fluage", Thèse de Doctorat, Université de Bourgogne, Juillet 1999.

[11] Kang and Anderson, "Neural Network application to the color scanner and printer calibrations", JEI 1, pp 125--134, 1992.

[12] Kröse B. J.A, Van Der Smagt P. P "A Introduction to Neural Networks", Seventh edition, Dec 1995

[13] Le Cun Y., "Modèles connexistes de l'apprentissage", Thèse de Doctorat, Paris 61987

[14] Maloney L.T., "Evaluation of linear models of surface spectral reflectance with small numbers of parameters", Journal Optical Society of America, vol 3, n°10, October 1986.

[15] Mancill C.E, "Digital color image restoration", PhD Thesis, University of Southern, California, 1975.

[16] Marquardt D, "An algorithm for Least-squares estimation of nonlinear parameters", SIAM J Appl. Math. 11, pp. 164-168, 1963.

[17] Norgaard, "System identification and Control with neural networks", Phd Thesis. departement of Automation, Technical University of Denmark (http :// www.iau.dtu.dk), 1996.

[18] Oukhellou L, "Paramétrisation et classification de signaux non destructif. Application à la reconnaissance des défauts de rails par courants de Foucault", Thèse de Docteur en Sciences, Université Paris XI Orsay, 1997.

[19] Peercy M.S., "linear color representation in full spectral rendering", Computer Graphics ACM Press, New York, pp 191-198.

[20] Ribes A., Schmitt F., Brettel H., "Reconstructing Spectral Reflectances with Neural Networks", The 3rd International Conference on Multispectral Color Science, June 18-20, 2001, Joensuu, Finland, see http://cs.joensuu.fi/mcs/preliminary_program.htm

[21] Rumelhart D.E., Hinton G. E., Williams R. J., "Learning internal representations by error propagation, in Parallel Distributed Processing : Explorations in the Microstructure of cognitive", Vol. 1 , MIT Press, Cambridge MA, pp 318-62, 1986.

[22] Shepherd A.J. "Seconds-Order Methods for neural Networks – Fast and Reliable training Methods for Multi-layer Perceptrons", Ed Springer, 1997.

[23] Smits B.E., Meyer G.W., "Newton's colors : simulating interference phenomena in realistic image synthesis", Eurographics Workshop on Photosimulation, Realism and Physics in Computer Graphics ,Springer Verlag, Berlin, pp 185-194, 1990

[24] Sun Y, Francchia F.D, Calvet T.W., Drew M, "Deriving spectra from colors and rendering light interference", IEEE Computer Graphics & Applications, n°16, pp 61-67, 1999.

[25] Dreyfus G, Martinez J.M, Samuelides M, Gordon M.B, Badran F, Thiria S, Hérault L , "Réseaux de neurones – méthodologie et applications", Ed. Eyrolles, 2001. http://www.neurones.espci.fr/

[26] Vapnik V.N, "The nature of statistical Learning Theory", Springer, 1995.

JOIN US AT THE NEXT EI!

IS&T International Symposium on

Electronic Imaging

SCIENCE AND TECHNOLOGY

Imaging across applications . . . Where industry and academia meet!

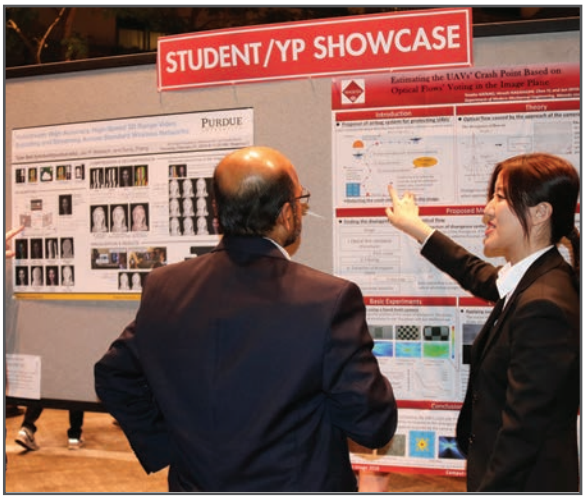

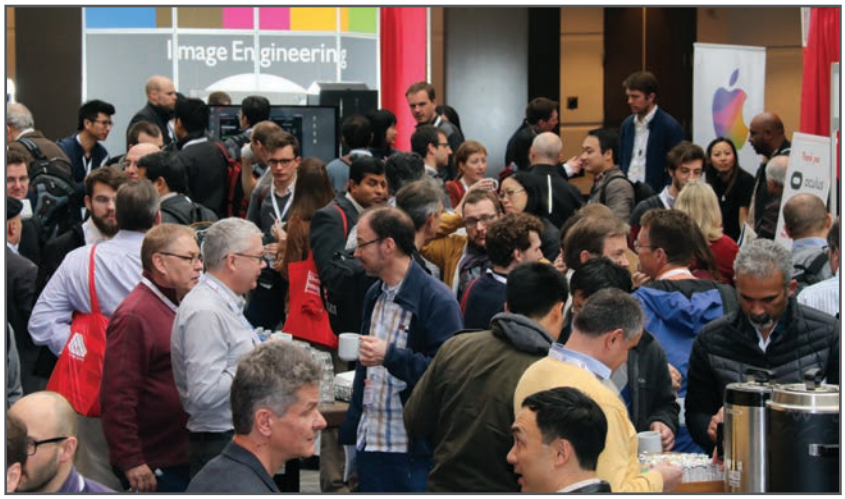

• SHORT COURSES • EXHIBITS • DEMONSTRATION SESSION • PLENARY TALKS •
• INTERACTIVE PAPER SESSION • SPECIAL EVENTS • TECHNICAL SESSIONS •

www.electronicimaging.org

IS&T
imaging.org